CDF/PUB/JET/PUBLIC/2645

RECENT RESULTS FROM QCD STUDIES AT CDF/D0 COLLABORATIONS

Anwar Ahmad Bhatti
for the CDF collaboration
Department of Physics
The Rockefeller University, New York
1230 York Avenue, New York, NY 10021

Abstract

The CDF and D0 Collaborations have collected 21.4 and 16.2 pb^{-1} of data, respectively, during 1992-93 collider run at the Tevatron at $\sqrt{s} = 1800$ GeV. The results on new compositeness limit using the inclusive jet cross section, and the energy flow within a jet are described. The fraction of jets originating from gluons is measured in the dijet and the photon+jet sample using a global likelihood method. The multiplicity, mass, transverse energy and angular distributions of multijet events are described. In all studies the results are compared to leading order and next-to-leading order QCD calculations and various QCD inspired Monte Carlo models. Results are found to be consistent with these predictions.

1 The Inclusive Jet Cross Section and Compositeness Limit

The measurement of the inclusive jet cross section provides a simple but a fundamental test of QCD. The theoretical uncertainty on the next-to-leading order ($\mathcal{O}(\alpha_s^3)$) calculation of the inclusive jet cross section is small for reasonable choices of the renormalization scale [1, 2]. Deviations from the standard model due to quark or gluon substructure are likely to be observed in large angle parton scattering, making studies of high E_T jets an attractive method to look for hints of new physics. At high E_T the jet production cross section is dominated by quark-quark scattering. The recent deep inelastic scattering experiments have made precise measurements of the structure functions F_2 and F_3. As a result, the quark distributions are known accurately at high x_{BJ}, the region which contributes to high E_T jet production.

The inclusive jet cross section is defined to be

$$\frac{1}{\Delta\eta}\int d\eta \frac{d\sigma}{dE_T d\eta} = \frac{1}{\Delta\eta}\frac{1}{\mathcal{L}}\frac{N_{jet}}{\Delta E_T}$$

where N_{jet} is the number of jets in the E_T range ΔE_T, $\mathcal{L}$ is the luminosity and $\Delta\eta$ is the η range of the data set used. In order to ensure that the energy is well measured, only those jets with the $|\eta_D|$ range 0.1–0.7 are used, where η_D is the pseudorapidity of the jet calculated under the assumption that the interaction took place at $z = 0$. The CDF central calorimeter covers $|\eta_D| < 1.1$[3].

We use a cone algorithm to reconstruct the jets[4] which is similar to the one used by next-to-leading order (NLO) QCD calculations[1]. The jet E_T is defined as the transverse component of the sum of the energy deposited by all the particles in a cone around the jet axis. In this analysis we use a cone of radius R=$\sqrt{\eta^2 + \phi^2} = 0.7$. The underlying energy (energy deposited by particles from fragmentation of spectator partons), measured using minimum bias events, is subtracted. The data are corrected for detector effects using the unsmearing procedure described in reference [5].

The measured cross section is in a good agreement with NLO QCD calculations using MRSD0′ parton distribution functions. The details of the comparison are described in reference[6]. In this paper, the data are used to calculate the lower limit on the compositeness parameter Λ_C. The effect of adding a term representing a flavour-diagonal contact interaction between quarks to the Leading Order QCD (LO) Lagrangian has been calculated in reference [7].

We use the MRSB0 parton distributions to evaluate the expected cross sections for various values of Λ_C. We scale the predicted cross section such that it agrees with the measured one in the range $95 < E_T < 145$ GeV, a region where the effect of a contact interaction is calculated to be small. The expected cross sections for different values of Λ_C divided by LO QCD cross section are shown in Fig. 1. The measured cross section, divided by LO QCD, is also superimposed. Comparing the predicted cross section with the data for $E_T > 200$ GeV, we calculate the compositeness parameter Λ_C to be larger than 1450 GeV at the 95% confidence level.

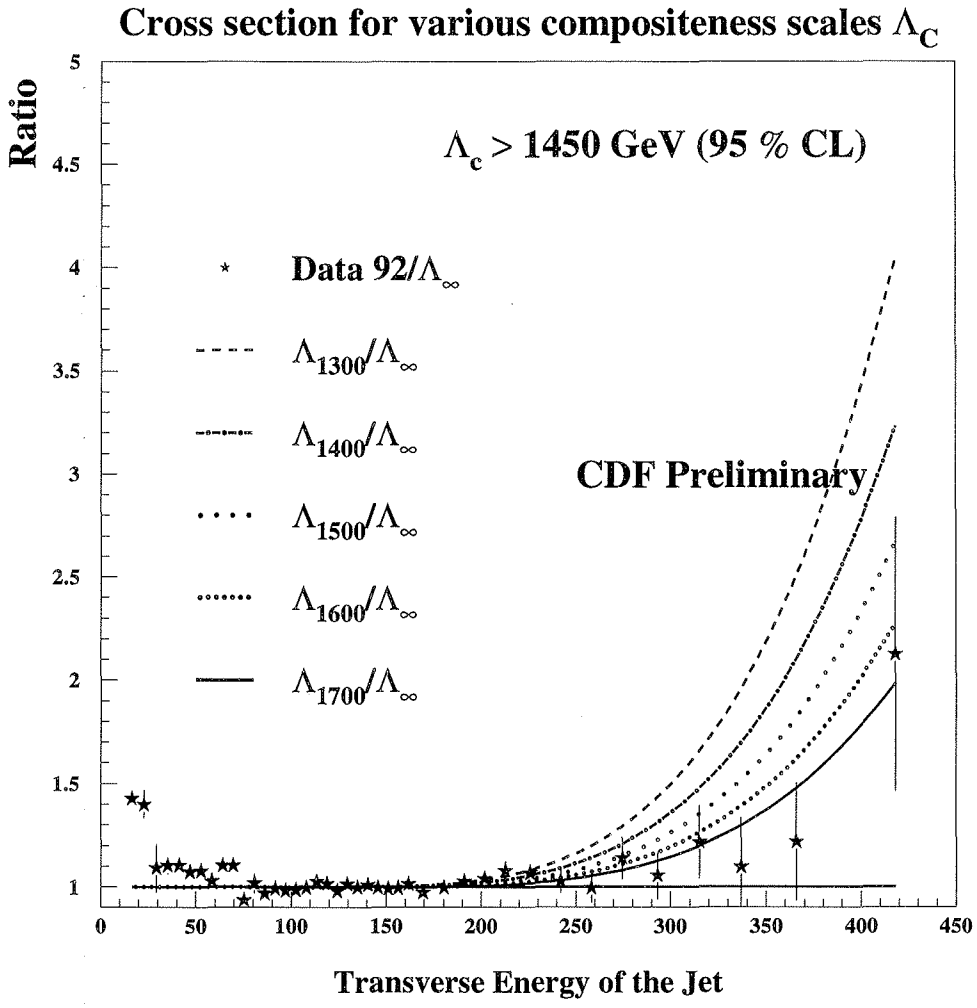

Figure 1: Comparison of Jet Cross Section with QCD+contact term predictions for various values of Λ_C.

2 Internal Structure of the Jets

As described in reference [6] the NLO QCD is successful in predicting the jet production cross sections, however fragmentation and hardonization of the partons is a complex process and the predictive power of QCD is limited, requiring the use of phenomenological models. Commonly used models include ISAJET[8] which is based on independent fragmentation; HERWIG[9] which is a parton shower Monte Carlo; and PYTHIA/JETSET[11] which is based on string fragmentation[10] and includes the parton showers for initial and final state partons. The $\mathcal{O}(\alpha_s^3)$ calculation[13] has also been used to describe the energy distribution inside a jet. Mathematically, the jet shape is defined by the average transverse energy density $\rho(r)$:

$$\rho(r) = \frac{\xi(r)}{\int_0^R \xi(r')dr'}$$

where

$$\xi(r) \equiv \frac{1}{\mathcal{N}_{jet}} \sum_{jets} \int_{E'_T > E'^{min}_T} \frac{E'_T}{E_T} \frac{d^2N}{dr dE'_T} dE'_T$$

and E'_T refers to the transverse energy of a tower in a jet and E_T is the total transverse energy of the jet in a cone of size R. The integral shape parameter $\Psi(r) = \int_0^r \rho(r')dr'$, is fraction of jet E_T deposited within a cone of size r where r is defines as $r = \sqrt{\Delta\eta^2 + \Delta\phi^2}$ with respect to jet axis[12].

The D0 collaboration has measured the energy flow within a jet using calorimetric information which has been corrected for detector effects. The clustering algorithm used is similar to the one described in [4] except D0 splits the overlapping clusters into two jets if they share less than 50% of the energy. Otherwise they are merged into a single jet. For this study, the clustering is done with a cone size $R = 1.0$. In Fig. 2 the shape parameter $\Psi(r)$ is plotted for several ranges of jet transverse energy. As expected the jets become more collimated as the energy of the jets increases. In Fig. 3 the jet shape parameter for jets with E_T in range 105-140 GeV is plotted. The jets are restricted to the pseudorapidity range $|\eta| < 0.2$. Predictions from various Monte Carlo models are superimposed. These different Monte Carlo models describe the shape quite well except perhaps at very small values of r.

The superimposed curves are based on $\mathcal{O}(\alpha_s^3)$ QCD calculation [13]. Using renormalization scale $\mu = E_T/4$ theory predicts that the jets are more collimated than what is experimentally observed whereas choice of $\mu = E_T$ gives a a better description. The difference between theory and data is further decreased by changing the jet merging procedure in the theory. The default procedure merges two partons into a single jet if they are less than a distance $R_{sep} = 2R$ apart. Changing this merging distance to 1.3 R, the agreement between the $\mathcal{O}(\alpha_s^3)$ theory and the data improves[13]. In reference [13] CDF data from 1988-89 run is compared with $\mathcal{O}(\alpha_s^3)$ for various values of merging distance and renormalization scale. In the CDF analysis from 1988-89 data[12], only the charge track information is used where as calorimetric information is used in the D0 analysis presented here.

3 Quark/Gluon Separation

The average particle multiplicity in a gluon jet is expected to be higher than in a quark jet because of different color factors associated with gluons and quarks. Naively, in the asymptotic limit $Q^2 \to \infty$, the ratio of multiplicities for quark and gluon jets is expected to be $< n >_g / < n >_q = 9/4$. However higher order corrections result in a smaller difference between quark and gluon jets[17]. At presently achievable Q^2 values, this asymptotic limit is not reached and the agreement with experiments is rather poor. Still the difference in their multiplicities can be used to statistically separate the quark and gluon jets. At the high E_T values, accessible at the Tevatron, the multiplicity is large and thus the differences between the quark and gluon jets is significant. We have used two Monte Carlo models HERWIG[9] and PYTHIA[11] to

predict the charge multiplicities and other properties of the quark and the gluon jets. Both of these models include the concept of planer color flow. The difference in the color flow associated with quark and gluon jets results in different fragmentation distributions.

We use dijet and photon+jet data sets for the quark/gluon separation analysis. The selection of dijet data is described in detail in reference [14] while photon+jet data and photon selection criteria are described in detail in [15]. The photon+jet includes the dijet background where one of the jets hadronizes into an isolated π^0, η or other mesons which decay into photons. The multiple photons coming from these mesons have higher probability of conversion in the material in front of the calorimeter and this background can be separated only on a statistical basis. We divide photon+jet into two sets, γ-enriched ("γ"+jet) and π^0-enriched ("π^0"+jet), based on the observed transverse electromagnetic shower profile.

At low E_T dijet data are expected to be dominated by $gg \rightarrow gg$ and $gq \rightarrow gq$ subprocesses. The leading order processes contributing to γ+jet events are $gq \rightarrow \gamma q$ and $q\bar{q} \rightarrow \gamma g$. The $gq \rightarrow \gamma q$ dominates the low E_T (x_{BJ}) events because of the larger gluon density and color factors. The "π^0"+jet data should look like the dijet sample.

The PYTHIA Monte Carlo predictions for the charged multiplicity distribution of the quark and gluon jets are shown in Fig. 4. A clear separation between the two types of the jets is predicted. The CDF dijet data lies closer to the gluons jets, though it has higher mean multiplicity than the predicted one. We have not made any attempt to tune the Monte Carlo to achieve a better agreement. As expected the photon+jet (including π^0, η background) lies in between the curves for the gluon and the quark jets.

The difference in the multiplicity distributions alone can be used to measure the fraction of jets originating from gluons. However, we have taken a step further and developed a likelihood method based on ten variables describing various properties of the jets. The method is described in detail in [16]. The variables include multiplicity, the electrical and mechanical moments of the longitudinal and transverse momenta of the particles and the electromagnetic fraction of the jets. The moments are defined as

$$\text{Longitudinal Mechanical Moments} = \sum_{i=1}^{n} (k_{L_i}/M)^m$$

$$\text{Transverse Mechanical Moments} = \sum_{i=1}^{n} (k_{T_i}/M)^m$$

$$\text{Longitudinal Electrical Moments} = \sum_{i=1}^{n} Q_i (k_{L_i}/M)^m$$

$$\text{Transverse Electrical Moments} = \sum_{i=1}^{n} Q_i (k_{T_i}/M)^m$$

where Q_i is the charge; and k_{L_i} and k_{T_i} are the longitudinal and transverse momenta of the ith particle with respect to jet axis and M is the invariant mass of the jet. Only the second moments, $m = \pm 2$, are used in this analysis.

As quark jets have smaller multiplicity, they are expected to have tracks with relatively higher mean momenta (for same E_T jets), thus making then more collimated. The gluon jets

contain more particles with lower mean momenta and therefore gluon jets tend to have higher fraction of energy deposited in electromagnetic calorimeter. We have used this likelihood method to find the gluon content of the jets in dijet events and photon+jet. As shown in Fig. 6 more than 80% of the jets in dijet sample are gluon jets at low E_T and the gluon fraction decreases with E_T. The superimposed curves are LO QCD calculation using MRSD0 and MRSD– parton distributions. The measured gluon fraction is higher than predicted, though within large systematic errors.

The gluon fraction measured in "γ"/"π^0"+jet events is shown in Fig. 7 using HERWIG and PYTHIA as references. As expected the gluon fraction in "π^0"+jet is found to be higher than "γ"+jet.

4 High ΣE_T Multijet Events

Within the framework of QCD, the high ΣE_T events are produced in hard parton-parton scattering. As shown in reference[6] LO and NLO QCD can predict the jet production rate quite successfully. Moreover we saw in Sec. 2, that internal structure of the jet and parton fragmentation is also successfully described by $\mathcal{O}\alpha_s^3$ QCD and QCD inspired Monte Carlo models. The next step is to study a system where multiple high E_T jets are produced. Experimentally these events can be selected by triggering on large ΣE_T where the sum is over all the clusters in the detector. These events are topologically complex and their study may help us understand higher order QCD processes.

The events were selected online by requiring event to have $\Sigma E_T > 300$ where the sum is over all clusters with $E_T > 10$ GeV reconstructed with CDF jet clustering algorithm[4] using a cone size $R = 0.7$. The cosmic rays and beam halo events are rejected by requiring missing E_T significance ($\not\!\!E_T/\sqrt{\Sigma E_T}$) to be less than 6.0. After the jet corrections the E_T cut is raised to 420 GeV to be fully efficient.

The jet multiplicity for jets with $E_T > 20$ GeV in with $|\eta| < 3.0$. is shown in Fig. 8(a). The data is in good agreement with predictions from HERWIG[9] events passed through CDF detector simulation for the jet multiplicities less than six. For higher jet multiplicities, HERWIG underestimates the rate. It is surprising that a leading order QCD parton shower Monte Carlo is able to describe the production rate up to five jets.

In Fig. 8(b), the mass for the multijet system is shown for $2, 3, 4, 5$ and 6 jet events. To ensure full acceptance, we require $\cos\theta^*$ to be less than 0.67 where θ^* is the angle between highest E_T jet and the beam direction in center of mass system. The histograms shown are the HERWIG predictions. Again we see that HERWIG describes the data quite well. The superimposed curves are from LO QCD parton level calculation of $2 \rightarrow 2$ and $2 \rightarrow 3$ processes (NJET)[18]. The MRSD0′ parameterization is used for the parton distributions and the renormalization scale is given by the average jet E_T. The multijet mass distributions are well described by both HERWIG and NJET calculation. In Fig. 9(a), the angular distributions of the hardest jet in the N-body rest frame are compared with Rutherford scattering, HERWIG

Monte Carlo and the NJET calculation. They are all similar to Rutherford scattering and are also well described by HERWIG. The transverse momentum distribution of the jets in the multijet events are shown in Fig. 9(b). The QCD parton shower Monte Carlo gives a reasonable description of the jet transverse momenta for two-jet events, but does not give an adequate description of three-jet and four-jet events. The full LO matrix element calculation NJET gives a good description of jet transverse momentum distribution for two-jet and three-jet events, thus perhaps probing the QCD matrix elements beyond the parton shower Monte Carlo approximation.

5 Conclusions

Using inclusive jet spectrum, we have measured the lower limit of 1450 GeV on the compositeness parameter Λ_C. Studying the energy distribution within a jet, we find that the jets become more collimated as the energy of jets increases. The shape of the jets is well described by the HERWIG, PYTHIA and ISAJET Monte Carlos. Using a likelihood method based on the charge multiplicity and various moments, we find that our dijet data is dominated by gluon jets. The γ+jet data has larger fraction of quark jets than the dijet data. Various distributions characterizing the multijet events are well described by HERWIG Monte Carlo and LO QCD predictions (where available), except the jet multiplicity distribution where HERWIG underestimates the ≥ 6 jet rate.

References

[1] S. Ellis. Z. Kunszt, and D. Soper, Phys. Rev. Lett. **62** 2188 (1989), Phys. Rev. Lett. **64** 2121 (1990).

[2] F. Aversa, P. Chiappetta, M. Greco, P. Guillet, Phys. Lett. B **210**, 225 (1988),**211**, 465 (1988); Nucl. Phys. **B327**, 105 (1989).

[3] CDF Collaboration, F. Abe *et. al.*, Nucl. Instrum. Methods **A271**, 387 (1988).

[4] CDF Collaboration, F. Abe *et. al.*, Phys. Rev. D **45** 1448 (1992).

[5] CDF Collaboration, F. Abe *et. al.*, Phys. Rev. Lett. **70** 1376 (1992) .

[6] Bernard Pope, "Jet and Direct Photon Production at D0 and CDF", contributed to these Proceedings.

[7] E. Eichten, K. Lane, and M. Peskin, Phys. Rev. Lett. **50**, 811 (1983).

[8] F. Paige and S.D. Protopopescu BNL report No. 38034 1986.

[9] G. Marchesini and B.R. Webber, Nucl. Phys. **B310**, 461 (1988); G. Marchesini *et al.*, Computer Phys. Comm. **67**, 465 (1992).

[10] B. Anderson, G. Gustafson and B. Soderberg, Z. Phys. C **1**, 105(1979)
B. Anderson, G. Gustafson and B. Soderberg, Z. Phys. C **20**, 317(1983).

[11] T. Sjotrand, Computer Phys. Comm. **39**, 347 (1986)
H.U. Bengtsson and T. Sjötrand, Computer Phys. Comm. **46**, 43 (1987).

[12] CDF Collaboration, F. Abe *et. al.*, Phys. Rev. Lett. **70** 713 (1993).

[13] S. Ellis. Z. Kunszt, and D. Soper, Phys. Rev. Lett. **69** 3615 (1992).

[14] CDF Collaboration, F. Abe *et al.* "Inclusive Jet and Two-Jet Differential Cross Sections at CDF" Submitted to 27th International Conference on High Energy Physics, Univ. of Glasgow, Glasgow, Scotland, July 20-27, 1994. FERMILAB-CONF-94/159-E.

[15] CDF Collaboration, F. Abe *et al.* "A Precision Measurement of the Prompt Photon Cross Section in $\bar{p}p$ Collisions" Submitted to 27th International Conference on High Energy Physics, Univ. of Glasgow, Glasgow, Scotland, July 20-27, 1994. FERMILAB-CONF-94/148-E.

[16] CDF Collaboration, F. Abe *et al.* "Jet Structure and Quark/Gluon Separation in CDF" Proc. 9th Topical Workshop on Proton-Antiproton Collider Physics, Univ. of Tsukuba, Tsukuba-Japan, oct. 18-22, 1993.

[17] A.H. Mueller, Nucl. Phys. **B241**, 141(1984);
J.B. Gaffney and A.H. Mueller Nucl. Phys. **B250**, 109(1985).

[18] W. Giele *et al.*, Snowmass 1990 Proceedings, page 137.

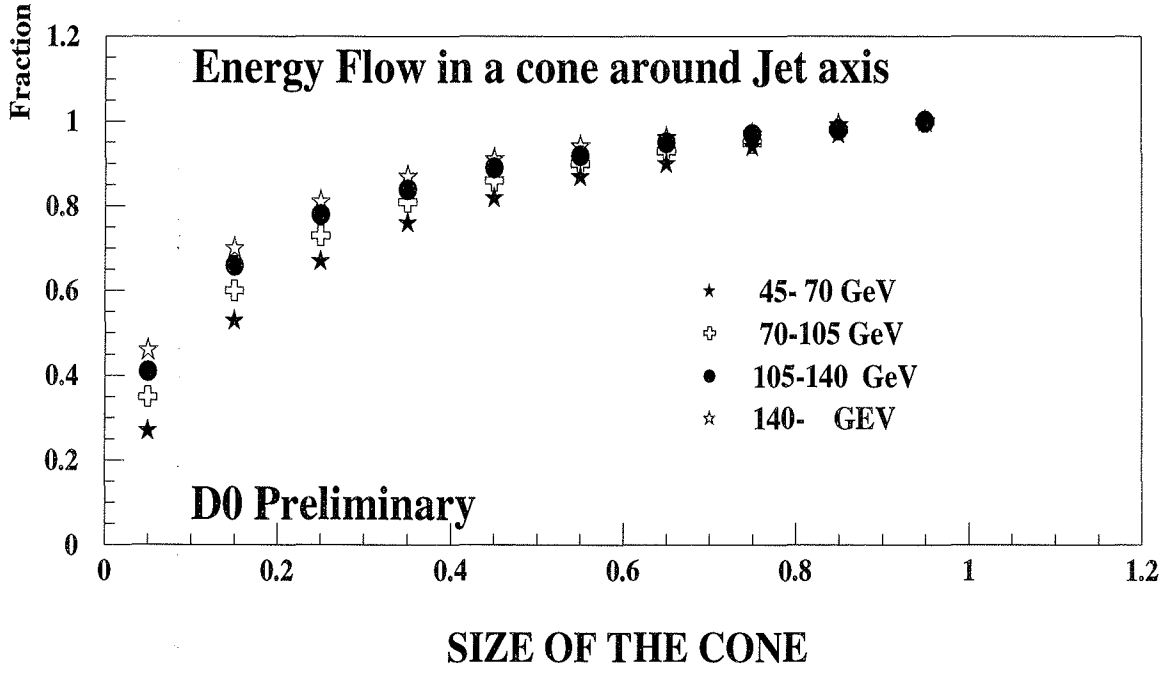

Figure 2: The integral energy flow in a cone around the jet axis showing the change in shape with jet E_T

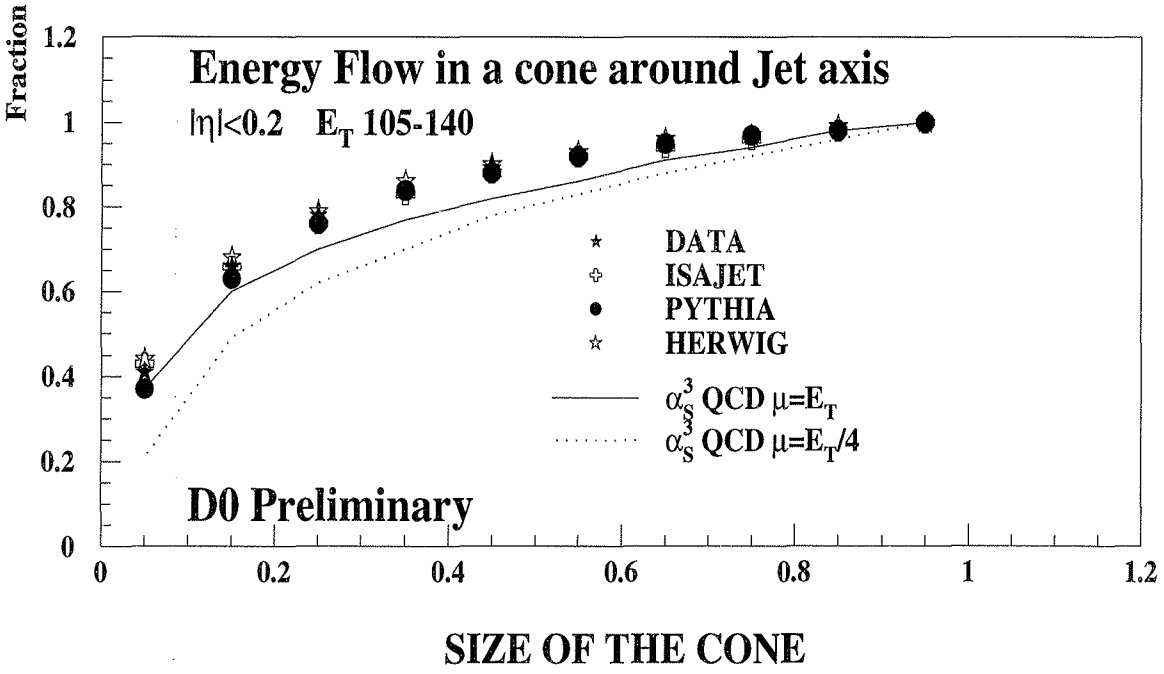

Figure 3: The integral energy flow in a cone around the jet axis compared with various predictions

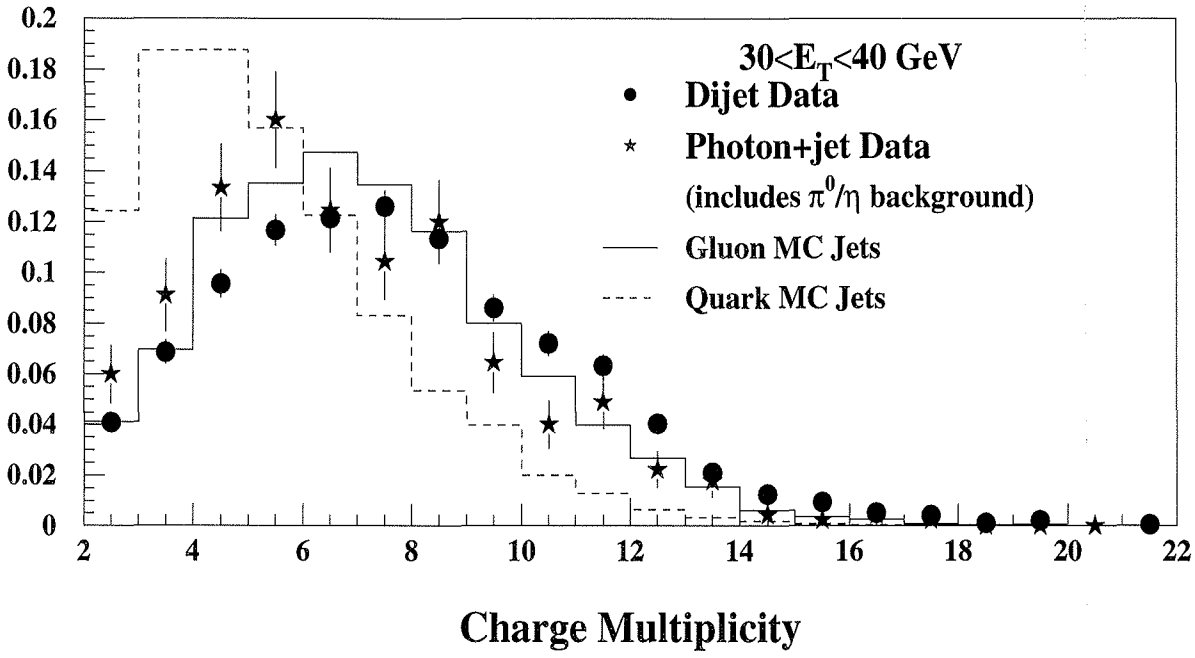

Figure 4: Charge particle distribution in a jet in dijet and direct γ+jet events as predicted by PYTHIA Monte Carlo. CDF dijet and photon+jet data are superimposed.

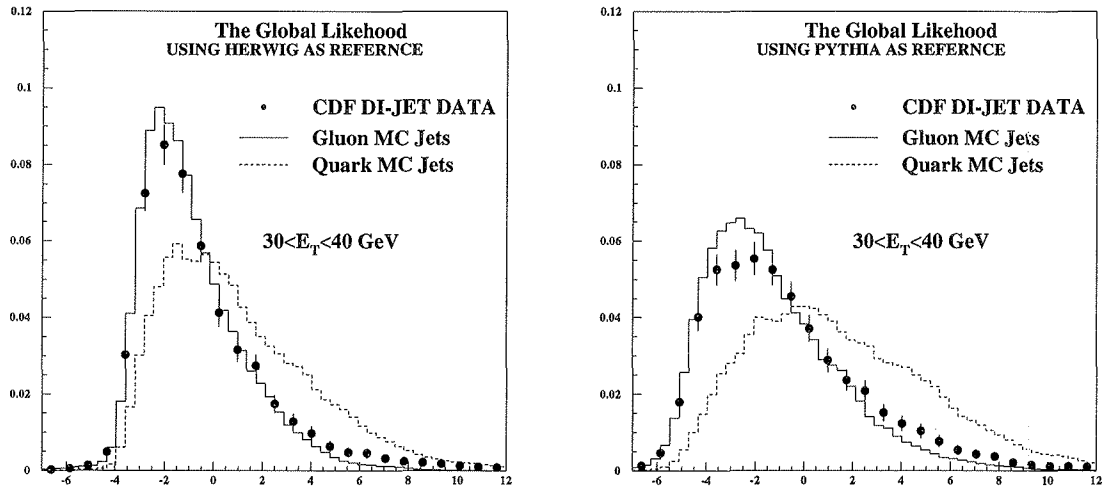

Figure 5: Global Likelihood distribution for dijet events using HERWIG and PYTHIA as the reference.

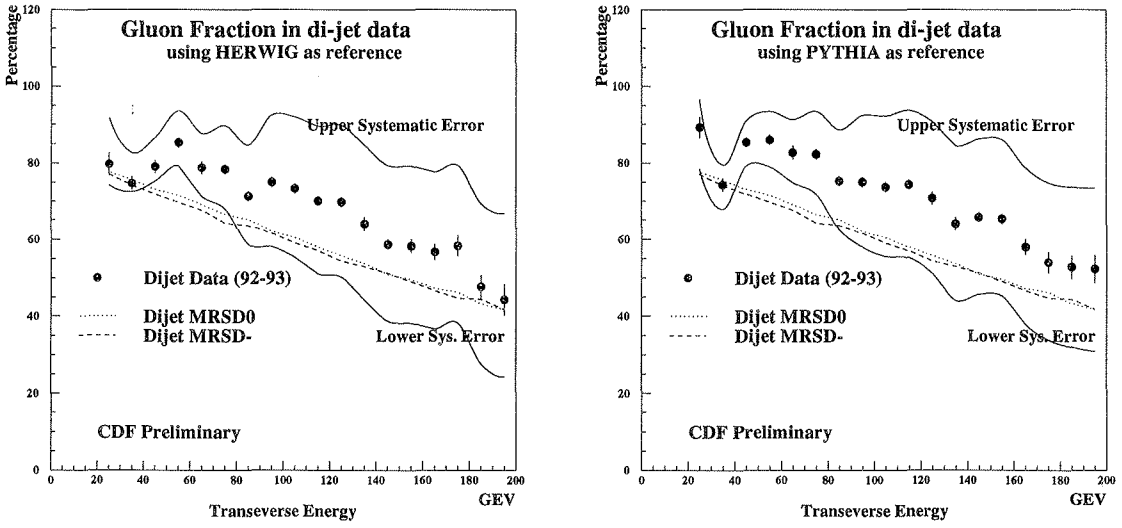

Figure 6: Fraction of jet originating from gluons in dijet data set using HERWIG and PYTHIA as the reference.

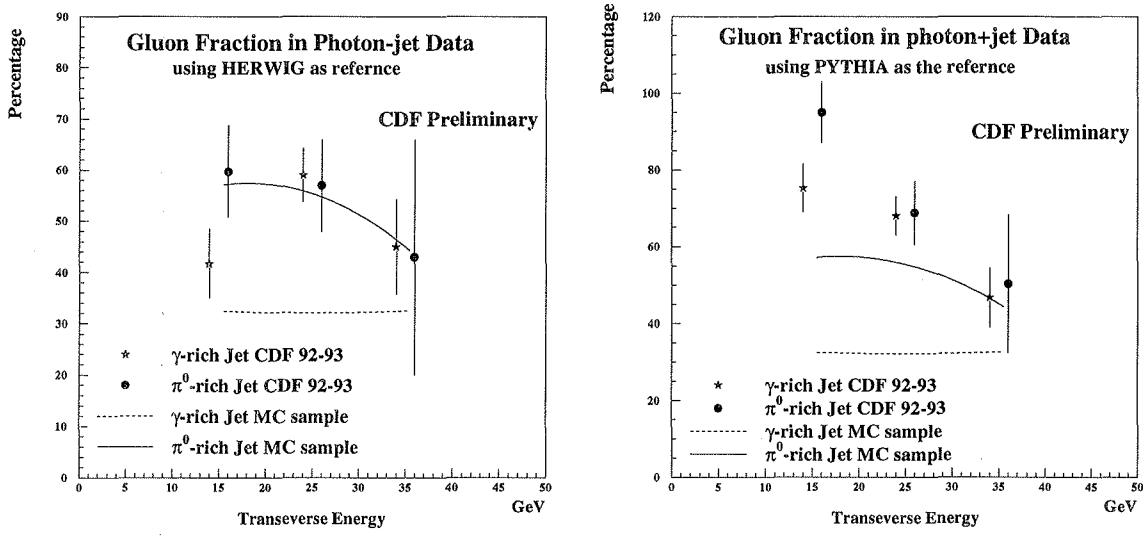

Figure 7: Fraction of jet originating from gluons in "γ"/"π^0"+jet data sets using HERWIG and PYTHIA as the reference.

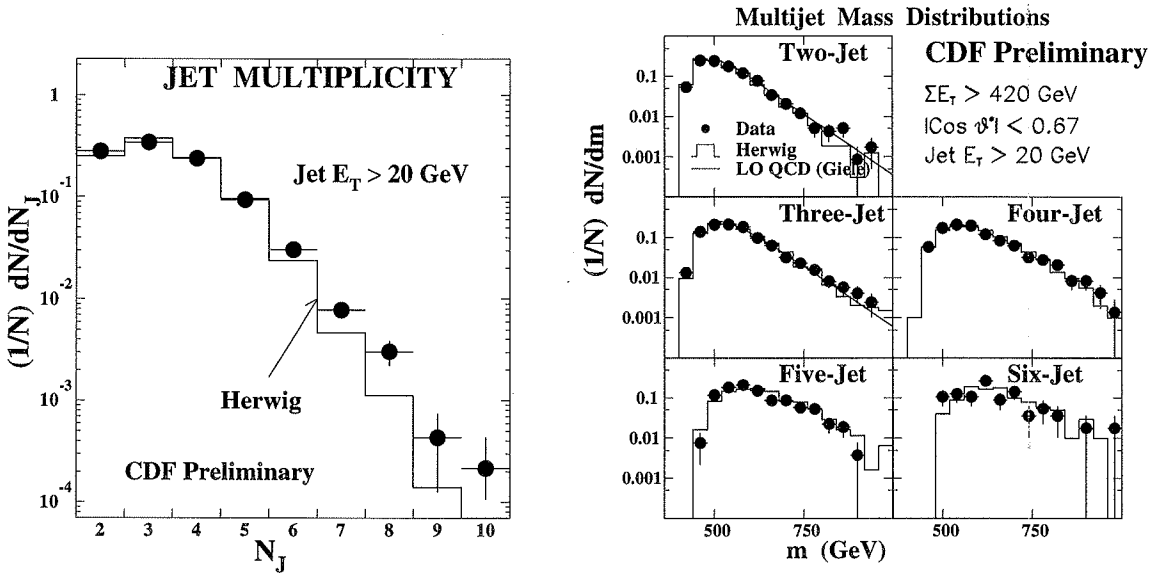

Figure 8: The number of jet and their mass distribution in high ΣE_T data set

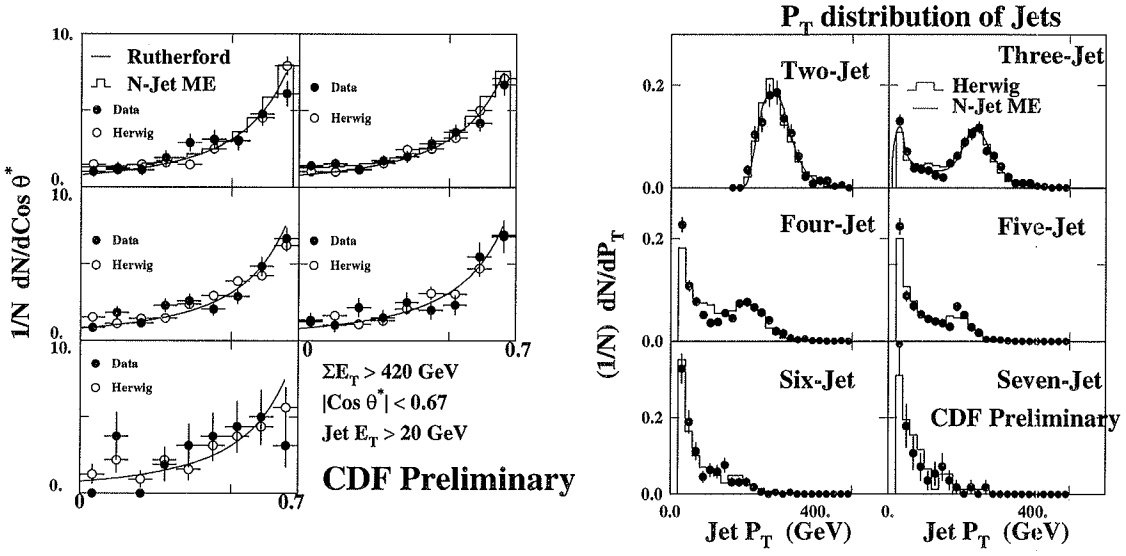

Figure 9: Angular and P_T distribution for multijet system